Trapped Free Radicals and Electrons in Organic Glasses

Low-temperature studies provide information on reaction intermediates of radiation chemistry.

John E. Willard

When molecules absorb appropriate amounts of energy, they fragment by rupture of bonds between atoms or by loss of electrons. Free radicals, electrons, and positive ions are produced (for example, $CH_3CH_3 \rightarrow 2CH_3$; $CH_3CH_3 \rightarrow CH_3CH_2 + H$; $CH_3CH_3 \rightarrow CH_3CH_3^+ + e^-$). The structures and reactions of the fragments are of basic interest and practical significance. In gases and liquids the lifetimes of these species are normally very short. Diffusion is rapid, and they combine with each other on nearly every encounter. Unless the temperature is low, the atoms and radicals may also react with stable molecules. Consequently, the steady-state concentrations which can be achieved for study are low. Rapid analysis after brief, intense pulses of activating radiation which produce momentarily high concentrations (1) has, however, made it possible to observe the optical spectra and reaction rates of species with half-lives as short as 10^{-11} second. Free radicals present at steady-state concentrations of about 10^{-7} molar during the continuous irradiation of liquid hydrocarbons with high-energy electrons have been studied by electron spin resonance (ESR), and the signal of solvated electrons in

The author is professor of chemistry at the University of Wisconsin, Madison 53706.

water has been seen by similar techniques (2). Low steady-state concentrations of atoms and radicals have also been observed by ESR in static and flow systems activated by visible, ultraviolet, and microwave radiation.

In contrast to the situation in the gaseous and liquid states, diffusion of radicals and ions in rigid glassy or crystalline matrices is so slow that they may not encounter each other for minutes, or even years, and reaction with matrix molecules may be precluded by activation energy barriers. In such systems the trapped species can be preserved for long times and studied at leisure by relatively simple techniques.

The present article surveys some of the current knowledge of the trapping of radicals, hydrogen atoms, and electrons produced in organic glasses by radiolysis and photolysis. Results in the field provide information on the spectra, identity, spatial distribution, and reaction kinetics of the trapped species and reveal previously unsuspected properties of the matrices, such as the ability of glassy hydrocarbons to trap electrons and positive charge.

The work before 1959 on the trapping of free radicals has been reviewed comprehensively (3). More recent reviews cover such topics as ionic processes in γ-irradiated solids (4), the radiation chemistry of organic solids

(5), reaction intermediates in organic solids (6), the radiation chemistry of frozen polar systems (7) and of frozen nonpolar and slightly polar systems (8), the spatial distribution of free radicals in irradiated solids (9), and free radicals and their reactions at low temperatures (10). Many studies of free radicals deposited on a cold finger after production in the gas phase, and examined by their infrared, visible, and ultraviolet spectra, have also been reported (11, 12).

Trapping and Detection of Radicals

Trapped free radicals are produced in any glassy organic materials exposed to x-rays, γ-rays, or high-energy electrons at temperatures near or below the glass transition temperature (viscosities of about 10^{12} poises or higher). Mechanisms of formation include decomposition of excited states (for example, $C_2H_6^* \rightarrow C_2H_5 + H$; the asterisk denotes an excited state); proton transfer ($C_2H_6^+ + C_2H_6 \rightarrow C_2H_7^+ + C_2H_5$); abstraction by hot atoms or radicals ($C_2H_6 + H^* \rightarrow C_2H_5 + H_2$); dissociative electron attachment ($CH_3I + e^- \rightarrow CH_3 + I^-$); and photolysis of the matrix or a solute. The yields of trapped radicals produced in organic solids by ionizing radiation are typically about three radicals per 100 electron volts absorbed; the quantum yields from ultraviolet irradiation are usually less than one. The radicals may be retained for years at a sufficiently low temperature, but they decay increasingly rapidly as the temperature is raised. In crystalline organic compounds, trapped radicals usually decay rapidly at temperatures above about 0.8 of the absolute melting point but are stable for days or years at lower temperatures.

Electron spin resonance spectroscopy is by far the most useful method for detecting and studying radicals trapped in organic solids. It is sensitive (to approximately $10^{-9}M$ radicals) and provides a theoretically predictable "finger-

print" for each type of radical. Although the line broadening that occurs in solids and the overlapping of spectra are limitations, they have not precluded studies of the products of radiolysis and their reactions. Early workers (*13*) have reported the spectra of radicals produced by irradiation at 77°K of many alkanes, olefins, alcohols, aldehydes, ketones, ethers, acids, esters, alkyl halides, and complex compounds of biological interest. Infrared analysis for organic radicals in organic matrices is generally precluded by the overlapping absorption bands of the matrix molecules. Visible-ultraviolet analysis has not been employed extensively with γ-irradiated organic glasses because of lack of knowledge of the spectra of radicals of the type formed and ambiguities introduced by competing absorptions from cations, carbanions, trapped electrons, and olefinic reaction products. The limitations are more severe in these systems than in those used for the characterization of many small free radicals by their optical spectra (*12*).

Decay of Radicals

The kinetics of the decay of radicals in rigid matrices are of three types. These reflect the spatial distributions of the radicals that result from the mechanisms by which they are formed (*5, 6, 14*).

One type is shown by methyl radicals produced from methyl halides (CH_3X, where X represents a chlorine, bromine, or iodine atom) by dissociative electron capture ($CH_3X + e^- \rightarrow CH_3 + X^-$) in glassy 3-methylpentane (3MP) at 77°K. The radicals decay by "pure" first order kinetics (the logarithm of the radical concentration is a linear function of time) with a half-life of 16 minutes (*14–16*). This is shown by the straight line of Fig. 1a. The first order kinetics require that each radical disappear by an event which is independent of the concentration of other radicals in the system. Events which meet this criterion are: (i) decomposition of the radical (this is ruled out by the known stability of the CH_3 radical); (ii) abstraction of hydrogen from a matrix molecule

($CH_3 + C_6H_{14} \rightarrow CH_4 + C_6H_{13}$); (iii) recombination of the radical with its original (geminate) partner ($CH_3 + X^- \rightarrow CH_3X^-$) before escape of either from the parent molecular cage in which they were formed. The abstraction reaction could occur in the glass at 77°K at the rate observed only if the activation energy is much lower than in the gas phase. In γ-irradiated 3MP glass containing CH_3X the CH_4 yield found after radical decay is much less than the initial CH_3 yield (*14*). This result is inconsistent with an abstraction mechanism and has led to interpretation of the decay of radicals in hydrocarbon and alkyl halide matrices in terms of the geminate recombination mechanism. Evidence for abstraction reactions in CH_3CN, CH_3NC, and CH_3OH matrices at 77°K is noted in a later section. Rearrangement of the radical to a geometry favorable for reaction must be the rate-controlling step since the rate of decay in 3MP is independent of whether the geminate partner is an iodide, bromide, or chloride ion (*14, 15*). The rearrangement appears to be controlled by thermal motions of the molecules in the walls of the cage or their substituent groups. Decay rates increase with increasing temperature.

With the exception of CH_3 radicals in 3MP, all the radicals produced by dissociative electron capture in all the matrices studied show fractional rates of decay, which decrease as the fraction decayed increases. This, the second of the three types of decay, is illustrated in Fig. 1a for CH_3 in 2-methylpentane and methylcyclohexane (*14*). The decay curves for samples that have received different doses, and hence have greatly different concentrations of radicals, are superimposable if plotted as the fraction of radicals remaining against time. This indicates that the fate of every radical is determined by combination with fragments from the same electron track, since it is unaffected by increasing the number of tracks. The decrease in the fractional rate of decay with increasing fraction decayed indicates that different members of the radical population have different probabilities per unit time of achieving the configuration necessary for recombination with the geminate partner, with which they are predestined to react. The decay rates decrease with increasing radical chain length, and sometimes change from one matrix to another in a direction opposite to the direction of change in viscosity (*14*). Such reac-
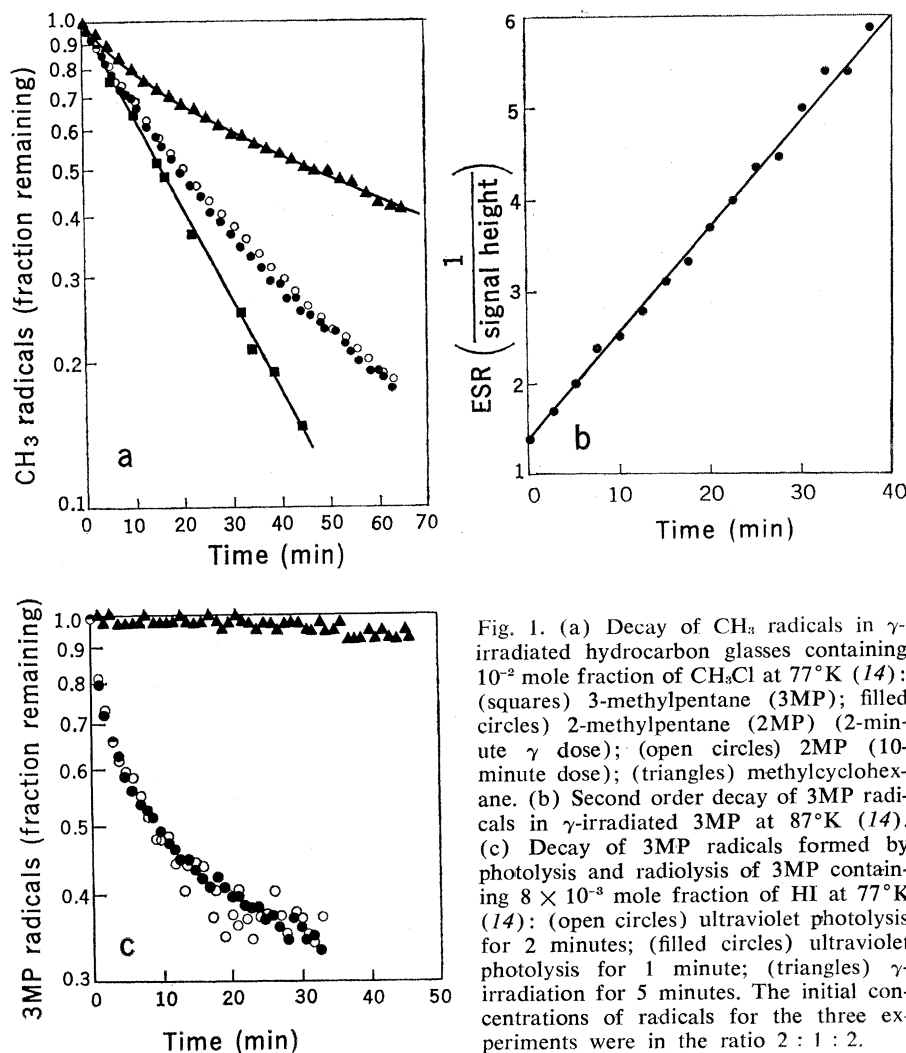

Fig. 1. (a) Decay of CH_3 radicals in γ-irradiated hydrocarbon glasses containing 10^{-2} mole fraction of CH_3Cl at 77°K (*14*): (squares) 3-methylpentane (3MP); filled circles) 2-methylpentane (2MP) (2-minute γ dose); (open circles) 2MP (10-minute dose); (triangles) methylcyclohexane. (b) Second order decay of 3MP radicals in γ-irradiated 3MP at 87°K (*14*). (c) Decay of 3MP radicals formed by photolysis and radiolysis of 3MP containing 8×10^{-3} mole fraction of HI at 77°K (*14*): (open circles) ultraviolet photolysis for 2 minutes; (filled circles) ultraviolet photolysis for 1 minute; (triangles) γ-irradiation for 5 minutes. The initial concentrations of radicals for the three experiments were in the ratio 2 : 1 : 2.

tions have been called "time-dependent first order" or "composite first order" reactions. They are first order in dose (initial concentration), but not in time. They may be viewed as governed by a continuum of first order rate constants determined by a continuum of types of restraints placed on the radicals by the matrix molecules.

Radicals which are not produced sufficiently close to a reaction partner to combine within the parent cage, spur, or track diffuse randomly in the matrix and combine with each other by second order kinetics. (The spurs are small volumes of high-density molecular fragmentation produced by the low-energy electrons ejected along the tracks of the primary, high-energy electrons which are ejected by the γ-rays.) This, the third type of radical decay, is illustrated by the decay at 87°K of the last approximately 50 percent of the 3-methylpentyl radicals produced by γ-irradiation of 3MP at 77°K (Fig. 1b) (14). The initial 50 percent decay by composite first order kinetics (17). These must react within the parent spur or track, whereas the radicals decaying by second order kinetics escape the parent track and react at random. A sharp contrast in rate of decay between 3-methylpentyl radicals produced in spurs with average distances between potential reaction partners of several molecular diameters or more and those born and retained within the same cage as their potential reaction partner is illustrated in Fig. 1c (14). The lower curve shows the decay of 3-methylpentyl radicals produced by abstraction of hydrogen from 3MP by hot hydrogen atoms from the photolysis of HI (HI + $h\nu$ → H* + I; H* + C_6H_{14} → C_6H_{13} + H_2; $h\nu$ denotes light). This process leaves the I atoms trapped adjacent to the C_6H_{13} radicals. The radicals combining with the atoms decay by composite first order kinetics, as shown by the superimposability of the normalized curves for different doses. This decay is much faster than that of an equal concentration of radicals produced by γ-irradiation (see upper curve of Fig. 1c).

Deuteration and Structure Effects

Deuterated radicals and protiated radicals with the same structure [for example, CD_3 and CH_3 (14); or C_2D_5, CD_3CH_2, CH_3CD_2, and C_2H_5 (18)], produced by dissociative electron capture in 3MP glass at 77°K decay at

equal rates. Deuteration of the matrix, however, causes a dramatic decrease in rate. The half-life of CH_3 and CD_3 radicals in C_6H_{14} (3MP-h_{14}) at 77°K is 16 minutes, and in C_6D_{14} (3MP-d_{14}) it is 150 minutes (14, 19). That of C_2H_5 is 300 minutes in C_6H_{14} and 1500 minutes in C_6D_{14} (14). All of the values are for matrices irradiated immediately after quench cooling at 77°K. The decay rates in matrices that have been allowed to stand for several hours at 77°K before irradiation are slower. The rates of decay of the four isotopic ethyl radicals in their respective parent matrices of ethyl iodide glass become progressively slower as deuteration of the matrices increases (Fig. 2a). The viscosities and molar densities of C_6H_{14} and C_6D_{14} are identical, within the accuracy of the determinations (20). Thus, it appears that differences in the rotational or vibrational frequencies of the molecules or their groups must control the rates of

recombination of the geminate pairs. Whatever the property of the matrix responsible for the matrix isotope effect, it plays a less important role as the temperature is raised; the rates of decay of methyl radicals in C_6H_{14} and C_6D_{14} approach equality at 87°K (14). Current work (21) indicates that the rates of decay of CH_3 radicals in C_6D_{14} glass at 77°K are different for different geminate partners (I⁻, Br⁻, Cl⁻), in contrast to the identity of decay rates in C_6H_{14}.

If, as postulated, the rate of radical decay is determined by the rate at which radicals retrieve the configuration necessary for combination with their geminate partners, it would be expected to vary for isomeric radicals of the same mass. Such an effect is observed for the isomeric butyl radicals formed from the isomeric butyl chlorides by dissociative electron capture in 3MP-d_{14} glass at 77°K (Fig. 2b) (18). However, differences dependent on
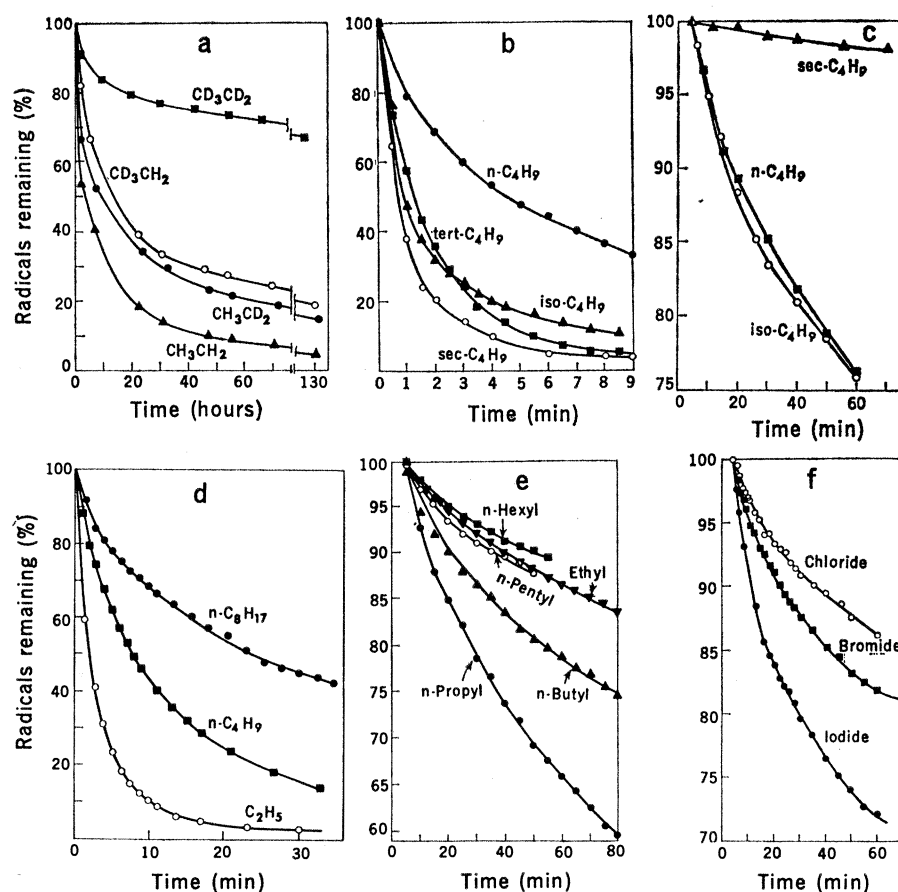

Fig. 2. (a) Decay of isotopic ethyl radicals in γ-irradiated glassy ethyl iodides at 77°K (18). (b) Decay at 87°K of isomeric butyl radicals formed by dissociative electron capture by 1 mole percent butyl chlorides in 3MP-d_{14} (18). (c) Decay at 77°K of isomeric butyl radicals in γ-irradiated glassy butyl chlorides (18). (d) Decay at 87°K of C_2H_5, n-C_4H_9, and n-C_8H_{17} radicals formed by dissociative electron capture by 1 mole percent alkyl iodides in 3MP-d_{11} (18). (e) Decay at 77°K of C_6H_{13}, C_5H_{11}, C_4H_9, C_3H_7, and C_2H_5 radicals in γ-irradiated glassy n-$C_6H_{13}Cl$, n-$C_5H_{11}Cl$, n-C_4H_9Cl, n-C_3H_7Cl, and C_2H_5Cl, respectively (18). (f) Decay at 77°K of C_5H_{11} radicals in glassy n-$C_5H_{11}Cl$, n-$C_5H_{11}Br$, and n-$C_5H_{11}I$ (18).

radical structure are outweighed by differences dependent on matrix structure when the latter is changed; the decay rate of secondary butyl radicals changes from slowest to fastest when the radicals are observed in matrices of their parent isomeric butyl chlorides (Fig. 2c) rather than in 3MP-d_{14}. Other structural effects on decay rates include a decrease in rate with increase of the chain length of radicals decaying in 3MP-d_{14} (Fig. 2d), a deviation from chain length dependence for ethyl radicals among radicals decaying in their parent alkyl chloride glass matrices (Fig. 2e), and a decrease in decay rate of ethyl radicals as the matrix is changed from ethyl chloride to bromide to iodide glass (Fig. 2f) (18).

In contrast to alkyl radicals produced by dissociative electron capture by alkyl halides in glassy alkanes and alkyl halides, methyl radicals in crystalline CH_3CN, CH_3NC, and glassy CH_3OH decay by abstraction of hydrogen from the matrix (22), forming CH_2CN, CH_2NC, and CH_2OH. The temperature dependence of the rates corresponds to activation energies of about 1 kilocalorie per mole, compared to approximately 10 kcal mole^{-1} in the gas phase, and there is a very large isotope effect, the rate being vanishingly small in the completely deuterated compounds. These abstraction reactions appear to result from quantum mechanical tunneling (22, 23), the only alternative being a reduction in activation energy resulting from changes in molecular configuration in the solids compared to the gases. Calculations for one-dimensional tunneling for different potential energy barriers support the tunneling hypothesis (23).

In crystalline organic compounds, where decay of trapped radicals is usually very slow at temperatures below about 0.8 of the absolute melting point, rapid decay sometimes occurs on warming through a solid-state transition which occurs at a much lower temperature (24). The decay is apparently aided by the structural and volume changes at the transition. The onset of decay is sharp in samples annealed at the transition temperature while cooling; but in quench-cooled samples, which may have islands of the high-temperature phase present in the low-temperature phase, it occurs below the transition temperature. In this range, decay proceeds rapidly on heating to each new temperature and
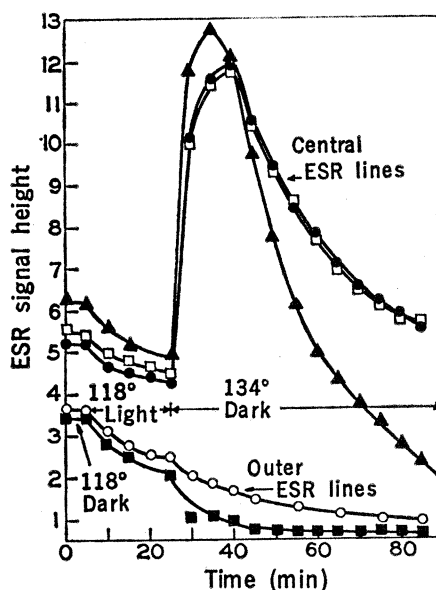

Fig. 3. Growth and decay of ESR signals attributed to C_2H_5 radicals in quench-frozen (77°K) γ-irradiated polycrystalline C_2H_5I when the temperature of the sample is raised to 134°K. The "central lines" are the C_2H_5 signal; the outer lines of the spectrum, which is 1000 gauss wide, are tentatively assigned to a species such as $C_2H_5I^+$, which yields C_2H_5 and I_2 on reaction with I^-. Each curve represents a different ESR line.

then falls to zero, which suggests a series of activation energies for the matrix equilibration processes that facilitate the decay (24).

Figure 3 illustrates two solid-state reactions that occur in γ-irradiated quench-cooled polycrystalline C_2H_5I when it is heated to 134°K (about 0.8 of its melting point). A complex ESR spectrum of more than 30 lines suddenly decreases in intensity, while the 6-line spectrum of the C_2H_5 radical grows rapidly and then decays (18). No such growth occurs in samples frozen slowly at the melting point (165°K) or in quench-cooled samples warmed to 145°K before irradiation at 77°K. It may be speculated that the growth is due to a reaction such as $C_2H_5I^+ + C_2H_5I^- \rightarrow 2C_2H_5 + I_2$, favored by structural reorganization in the strained samples. In the absence of strain the reaction occurs at higher temperatures, where the C_2H_5 radicals decay too rapidly to be observed.

Differences in crystal structure of otherwise similar matrices sometimes cause major differences in the relative stability of different reaction intermediates. This is illustrated by the "odd-even effect" in γ-irradiated polycrystalline alkyl iodides. In the glassy state all of the iodides give the ESR spec-

trum of the corresponding alkyl radical. The polycrystalline iodides with an uneven number of carbon atoms (C_3, C_5, C_7) also give the alkyl radical signal, but the polycrystalline C_2, C_4, C_6, and C_8 iodides give completely different and more complex spectra, which must involve the interaction of unpaired electrons with iodine nuclei (25).

Other examples of the sensitivity of reaction pathways to matrix structure include: (i) the formation of isobutyl radicals in the glassy state as contrasted to tertiary butyl radicals in the polycrystalline state, when mixtures of 92 mole percent isobutane and 8 mole percent 3MP are irradiated at 77°K (26); (ii) radical formation predominantly by the rupture of secondary C–H bonds rather than the weaker tertiary or more abundant primary bonds when glassy 3-methyl alkanes are exposed to γ-irradiation, hot atom attack, hot radical attack, or photosensitization by aromatic solutes (27); and (iii) other unexpected bond selectivity effects in 2-methyl alkanes (10, 28).

In γ-irradiated 3MP glass containing dissolved O_2 or Cl_2 at 77°K, the spectrum of the 3-methylpentyl radical gradually changes to that of the peroxy radical in the case of O_2, and to a spectrum attributed to a complex between a 3-methylpentyl radical and a chlorine molecule in the case of Cl_2. The rates of reaction have been used to estimate the diffusion coefficients of the O_2 and Cl_2 in the matrix (29). A similar conversion of alkyl radicals to peroxy radicals was observed when radicals formed in a rotating cryostat were exposed to gaseous O_2 (10).

Growth of Radicals

During γ-irradiation of glassy hydrocarbons the concentration of trapped radicals grows in direct proportion to the dose up to radical concentrations of at least $5 \times 10^{-4}M$ (30). In other matrices—including ethylene glycol (31), C_2H_5I (32), and C_2Br_6 (33)—the rate of growth decreases with increasing dose. For example, the rate of Br_2 production during γ-radiolysis of C_2Br_6 decreases by a factor of 10 as the dose is increased from 0.2×10^{19} to 5×10^{19} electron volts per gram. One interpretation of this decrease is that radicals are preferentially formed near defect sites where other radicals

have already been formed, with each cluster disappearing by combination when it reaches a critical size (*31*). In another model it is assumed that the radicals are formed in conventionally distributed tracks and spurs and that radiation-catalyzed removal of radicals occurs because energy or charge deposited in the matrix during continuing irradiation migrates, encounters the spurs, and hastens radical recombination within them (*32*). A model has been developed for the quantitative evaluation of the competing growth and decay reactions (*34*).

Distances between Radicals

Irradiated oximes (*28*), polymers (*35*), crystalline normal alkanes, and glassy squalane ($C_{30}H_{62}$) (*36*) give ESR signals of transitions characteristic of the triplet state of radical pairs with separations between pair partners of 5 angstroms to 7 angstroms. In these characteristic transitions the spin magnetic quantum number M_s changes by 2: $\Delta M_s = 2$. Pair formation relative to the production of isolated radicals varies with the chain length and other properties of the matrix. The most probable mechanisms for pair formation appear to be (i) ejection of a hot hydrogen atom from a C–H bond, followed by its attack on an adjacent molecule to form H_2; and (ii) proton transfer to an adjacent molecule ($RH^+ + RH \rightarrow R + RH_2^+$, where R is a group such as C_6H_{13} from the C_6H_{14} molecule), followed by the reaction $RH_2^+ + e^- \rightarrow R + H_2$. First order kinetics have been reported for decay of radicals in polymers, as expected for decay by recombination with geminate partners (*37*).

There is little evidence on ESR signals corresponding to triplet state transitions with $\Delta M_s = 2$ from ion pairs, although this would be of great interest. It appears that the ESR spectrum of γ-irradiated single crystals of maleic anhydride can be explained in terms of species formed by electron transfer, but not by neutral radicals (*38*).

The high-energy electrons (averaging approximately 5×10^5 ev for ^{60}Co) ejected by γ-rays are believed to dissipate their energy by ejecting electrons of much lower energy (approximately 100 ev) at intervals of 1000 Å or so along the electron track. The low-energy electrons excite and ionize molecules within a relatively small vol-

ume, the spur. Studies of saturation of the ESR signals of trapped electrons have been used to make estimates of the maximum size of the spurs by determining the γ dose at which the relaxation time [$(T_1 T_2)^{0.5}$, where T_1 is the spin-lattice relaxation time and T_2 the spin-spin relaxation time] begins to decrease as a result of spin-spin relaxation between electrons from different spurs. For trapped electrons in 3MP glass, the data imply spur radii of more than 130 Å, and in methyltetrahydrofuran (MTHF) radii of more than 63 Å are inferred (*39*). Similar data obtained from ESR spectra of free radicals show relaxation times at low doses which are shorter than those for electrons and do not change at the highest doses tested. This suggests the possibility that many of the radicals are formed in pairs.

Photochemical Reactions of Radicals

Potentially, the trapping of radicals at substantial concentrations in rigid matrices opens the way to a study of photochemically activated reactions of such radicals. Examples of such reactions include the isomerization of tertiary butyl radicals to isobutyl radicals in γ-irradiated isobutyl bromide at 77°K, and photoinduced radical conversions in polymers; also, enhanced yields of certain products are obtained from alcohols exposed to ultraviolet light at 77°K following γ-irradiation (*40*). Progress in the field has been hindered by lack of knowledge of the optical absorption spectra of free radicals, and the difficulty of determining these in γ-irradiated systems because of interference from overlapping spectra of carbanions, cations, trapped electrons, and radiation-produced olefins.

Trapped Hydrogen Atoms

Trapped hydrogen atoms produced by γ-irradiation of methane at 4°K (*41*) are stable for hours at that temperature but disappear on warming to 30°K (*42*). Systematic attempts to produce them by the γ-irradiation of other rigid hydrocarbons at 4°K or above have given negative results (*42*), but they can be produced by photolysis of HI in perdeuterated 3MP at 50°K or below. The kinetics of their growth and decay suggest that the rate-controlling step is the detrapping, and that

retrapping is improbable (*43*). The absence of trapped H atoms in radiolyzed 3MP-d_{14} containing HI, whereas the ESR signal of the H atom appears when the HI is photolyzed, indicates that radiolysis of the solid does not produce H atoms or, if it does, that they all react with matrix molecules to form HD, or are of too low energy to be trapped (*43*). In contrast to the photolysis of HI in 3MP-d_{14}, no trapped H atoms are formed when HI is photolyzed in 3MP-h_{14}. This matrix isotope effect is due to a reduction in the yield of thermal H atoms because the photochemically produced H atoms can abstract H from C–H bonds more readily than D from C–D bonds (*44*).

Several investigators have observed and studied trapped H atoms in acidic ices at 77°K and below (*45*).

Electron Trapping

Electrons produced in a medium by ionization of its molecules may have only a transitory existence before recombination with the positive ions, or these free (mobile) electrons may become stabilized by nonspecific interactions with groups of surrounding molecules. The lifetimes of stabilized electrons (*46*) range from years for solvated electrons produced by the addition of alkali metals to compounds such as liquid ammonia and for "F" centers in alkali halide crystals, to microseconds for electrons in irradiated liquid water (*47*) and in liquid alcohols and hydrocarbons (*48*).

In the glassy state of many organic materials at low temperatures, trapped electrons are stable for days. Concentrations as high as 10^{17} g^{-1} in 3MP (*49*) and 10^{19} g^{-1} in ethanol (*50*) have been observed after γ-irradiation. The techniques by which they can be investigated include ESR and optical spectroscopy, thermally and photochemically stimulated luminescence, and electrical conductivity (*4–6*). Elucidation of the nature of the potential wells that prevent the electrons from migrating rapidly to the equal populations of cations in the matrices now challenges investigators. Questions to which answers are being sought experimentally include: Do the matrices contain preformed trapping sites, or does the electron "dig its own hole" by orienting molecules by polarization forces? What trap depths are indicated

by the wavelengths capable of producing photobleaching? Are all traps in a given matrix of the same depth? Do they have bound excited states to which the electrons can be raised without being detrapped? Do electrons react with the cation population at random, or only with their geminate cations? Can trapped electrons tunnel to cations and scavenger molecules?

Nature of Electron Traps

Pulse radiolysis studies (51, 52) and effects of temperature on the optical and ESR spectra (53, 54) of electrons produced in organic glasses at 77°K and below indicate that they are trapped in less than 10^{-7} second, but that the initial trapping environments are subsequently altered by the polarization forces. The absorption spectrum of electrons in glassy ethanol immediately after a 12-nanosecond radiation pulse at 77°K (Fig. 4A) is dramatically decreased at the longer wavelengths and increased at the shorter (solid line of Fig. 4A) after 4 microseconds. This suggests an increase in the energy of
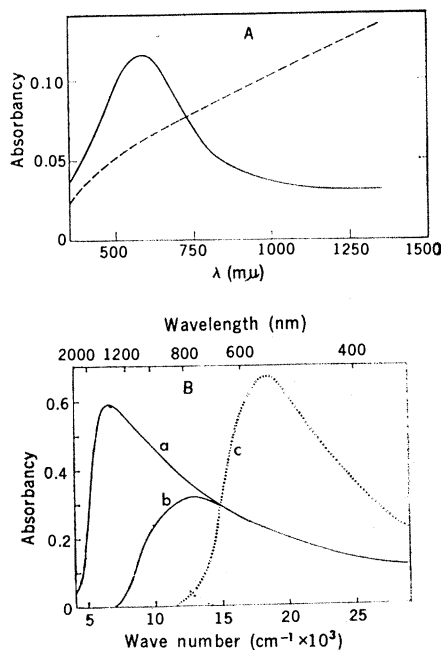

Fig. 4. (A) Transient absorption spectra of trapped electrons following pulse radiolysis (12 nsec) of ethanol glasses at 77°K (51): (dashed line) spectrum at the end of the pulse; (solid line) spectrum after 4 μsec. (B) Absorption spectra of trapped electrons in ethanol glass at 4°K after γ-irradiation at 4°K (53). Spectrum a was obtained before photobleaching and spectrum b after bleaching with 1200-nm radiation. Spectrum c was obtained when irradiation and measurement were done at 77°K with the same γ dose used at 4°K.

binding of the electrons, resulting from orientation of the dipolar alcohol molecules in the walls of the traps. Irradiation of ethanol glass at 4°K induces a stable spectrum (Fig. 4B), qualitatively identical with the initial transient spectrum in the pulse experiments at 77°K. The electrons responsible for this spectrum must be trapped in sites present before irradiation, since rapid orientation of dipoles is precluded at 4°K. Photobleaching at long wavelengths appears to detrap selectively the more weakly trapped electrons (Fig. 4B). When samples irradiated at 4°K are warmed to 77°K the spectrum shifts (53) to that obtained when the irradiation is done at 77°K; this indicates that, as the matrix softens, the polarization forces are able to deepen the traps.

In agreement with the evidence from optical spectra, the ESR line of trapped electrons in ethanol irradiated and observed at 4°K is much narrower (6.7 gauss) (54) than that for irradiation and measurement at 77°K (14 gauss). Variations in both the optical and ESR spectra with the nature of the medium indicate that the trapped electron interacts with the surrounding nuclei. The maximum of the optical absorption band shifts to shorter wavelengths (Fig. 5a) and the ESR line width broadens (Fig. 5b) as the polarity of the matrix increases (55). The ESR line width in C_2H_5OH glass at 77°K is 14 gauss and that in C_2H_5OD glass at 77°K is 6 gauss (54, 56), indicating that the molecules in the walls of the traps are predominately oriented with their hydroxyl groups toward the electrons. Glassy mixtures of isopropyl alcohol and ethylene glycol (static dielectric constants 18.6 and 37.7) show a single optical absorption curve for each composition, which shifts to the blue and narrows with increasing ethylene glycol concentration, suggesting a random orientation of the two types of molecules in the walls of the trapping site. By contrast, in mixtures of n-propyl alcohol and 3MP the two peaks characteristic of the independent solvents are found, suggesting aggregation of the alcohol molecules (55). The optical absorption spectrum of trapped electrons in C_2H_5OH glass at 77°K is similar to the spectrum of solvated electrons in liquid ethanol, except that it is narrower and shifted to shorter wavelengths (55, 57). This suggests that the electrons are held in similar molecular cages in the two media, the volume being smaller in the glass. The

much shorter lifetime of the electron in the liquid is presumably due to a combination of thermal turnover of the cage structure, rapid diffusion to cations, and chemical reaction with C_2H_5OH.

The stable optical spectra of trapped electrons observed after relaxation of the dipolar environment at 77°K (Figs. 4 and 6) might result from: (i) a continuum of trap depths, with only photons of energy in excess of the trap depth being absorbed; (ii) uniform trap depths, with the threshold energy for detrapping being at the long-wavelength end of the spectrum; or (iii) traps with bound excited states accounting for absorption at the longer wavelengths of the spectrum, with the photothreshold for detrapping being at lower wavelengths. If there were a continuum of trap depths, changes in spectral shape might be expected during thermal decay and during photobleaching with selected wavelengths of monochromatic light. Slight shifts have been reported (50, 58), but they are small, suggesting that all traps in the
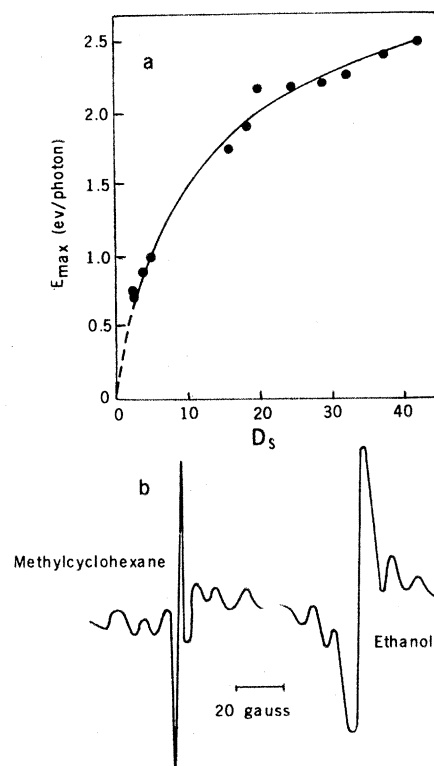

Fig. 5. (a) Photon energy (E_{max}) at the maximum of the optical absorption spectrum of trapped electrons at 77°K as a function of the static dielectric constant (D_s) of the organic matrices. The matrices ranged from 3MP ($D_s = 2$) to glycerol ($D_s = 43$). (b) Electron spin resonance spectra at 77°K of trapped electrons in glassy methylcyclohexane and glassy ethanol (55). In each case the central singlet is the electron signal.

same medium are very similar. Photo-bleaching thresholds of approximately 1.4 and 0.75 ev have been indicated for detrapping of electrons in glassy MTHF (58) and 3MP (59), respectively. In each case the spectrum extends to much lower energies, this portion being attributed to absorption which results in exciting electrons to bound excited states of the traps. There is evidence that in MTHF an electron in a bound excited state may absorb a second photon which detraps it, producing bleaching and photoconductivity (60). For 3MP there is new evidence that the detrapping threshold is about 0.53 rather than 0.75 ev (61). The initial quantum yield for bleaching rises continuously from about 10^{-2} at 0.53 ev to higher values at shorter wavelengths, suggesting that the probability of a detrapped electron "finding" a cation rather than being retrapped may increase with the amount of energy it is given in excess of the trapping energy. During photobleaching of the first 50 percent of the trapped electrons in MTHF glass, the relative quantum yields for bleaching decrease by a factor of 20 (58). In 3MP glass the absolute quantum yields decrease from 0.8 to 0.3 during bleaching of the first 50 percent of the electrons (59). These interesting changes have not yet been satisfactorily explained.

Spatial Distribution of Traps

As with the free radicals discussed in an earlier section, trapped electrons produced by γ-irradiation of an organic glass might be expected to be present in spurs, that is, in local concentrations higher than the average concentration in the system. Estimates of the average distance of separation of the electrons from other entities with unpaired spins, made from studies of the power saturation characteristics of the ESR signal, yield values of 40 to 50 Å (62) and 60 Å (39) in MTHF, more than 130 Å in 3MP, and 100 Å in triethylamine (39). They suggest that the electrons are more dispersed than the free radicals, and that the separation increases with decreasing polarity of the matrix (39).

Three types of evidence indicate that each electron is trapped so close to a particular positive ion that it must inevitably combine with that ion. One is that the fraction of the electrons that decay per unit time after a short irradiation is independent of the inten-
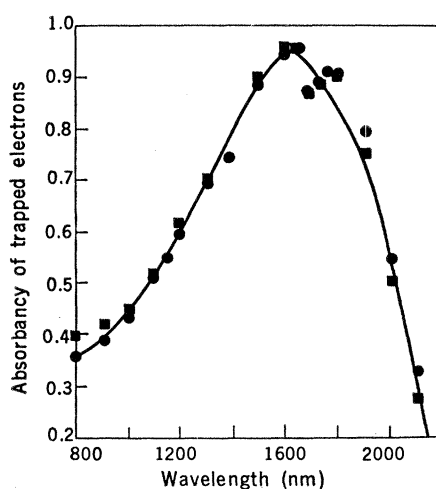
Fig. 6. Absorption spectra of trapped electrons in γ-irradiated 3MP at 77°K. (Circles) Five minutes after irradiation; (squares) 45 minutes after irradiation, when approximately 50 percent of the electrons had decayed. The absorbancies for the two spectra were normalized at 1560 nm (81).

sity of the irradiation and hence of the concentration of electrons and cations (5, 6). The decay curves for samples with widely different doses are superimposable after normalization for dose. Similarly, the decrease in the quantum yield for photobleaching with increasing fraction bleached is independent of the initial electron concentration (58). The second type of evidence for geminate recombination comes from observation of the polarization of the fluorescence emitted when electrons produced in 3MP glass by photoionization of a solute by vertically polarized light are photobleached in the presence of a large population of cations produced by horizontally polarized light (63).

The fluorescence is predominately vertically polarized. The solute used was tetramethyl-p-phenylenediamine (TMPD). The trapped electrons produced from it give the same optical and ESR spectra and decay rates as those produced by γ-irradiation (64), indicating that the characteristics of the electron traps in glasses are not dependent on the nature of the cation. Studies with TMPD have given additional evidence for geminate pair trapping; that is, the application of an electric field to a photoionized sample produces a burst of luminescence which is not repeated by a second application with the same polarity, but is repeated when the polarity is reversed before the second application (65). This is interpreted as indicating that all electrons are trapped within the Coulomb field of the geminate cat-

ion and that, for those on the negative side of the cation relative to the applied potential, the potential couples with the Coulomb force of the cation in overcoming the potential barrier of the trap in the direction of the cation. It is concluded from the data that the trapped electrons are distributed in the range of 10 to 50 Å from the cations.

Evidence for Electron Tunneling

There has been a problem (5, 6, 66) of reconciling the concept of geminate pair trapping with evidence that electrons produced by γ-irradiation or photoionization travel thousands of angstroms before being trapped. The long ranges are implied by the efficiency of electron scavenging solutes, which compete for electrons that would otherwise be trapped; for example, 10^{-3} mole fraction of biphenyl in 3MP glass reduces the yield of trapped electrons almost to zero (4, 67). Correlation of the two seemingly contradictory lines of evidence appears to be provided by evidence (66, 68) that nearly all newly produced electrons are trapped before being scavenged, and that the scavenging process occurs as a result of subsequent tunneling to scavenger molecules which have a greater electron affinity than the trap depth. In matrices where no decay of trapped electrons occurs in the absence of a scavenger, transfer from traps to scavenger molecules has been observed over a time scale of 1 μsec to 10 minutes; the kinetics observed are as predicted for a tunneling process, approximately equal concentrations decaying per order of magnitude increase in time. Other evidence that indicates tunneling includes: (i) the enhancement of the yield of the anion of a scavenger of high electron affinity as the concentration of a scavenger of lower electron affinity is increased (66); (ii) temperature-independent isothermal luminescence decay rates in γ-irradiated organic glasses over the range from 4° to 77°K (69); (iii) the evaluation of a tunneling model for organic glasses and of decay rates of trapped electrons and oxide anions (O$^-$) in irradiated 10M NaOH glasses (70); and (iv) the reactivities of electrons in ethylene glycol–water glass (71).

During γ-irradiation of organic glasses the concentration of trapped electrons increases, passes through a maximum, and then falls gradually toward zero (72). In the meantime the

concentration of trapped radicals continues to grow nearly linearly. The decrease in the concentration of trapped electrons is thought to be due to the increasing probability of tunneling to a radical as the radical concentration increases (66). The radicals are believed to act as electron scavengers forming carbanions. Assuming that three free radicals are produced per 100 ev absorbed, and that they are uniformly distributed, the average distance between trapped radicals in a glass that has received a dose at which the concentration of trapped electrons begins to decrease is approximately 13 molecular diameters, and the average distance of an electron from a radical is approximately five molecular diameters (about 25 Å). In the same system the average distance of electrons from trapped cations, assuming uniform spacing of the latter, is approximately six molecular diameters. At this distance the Coulomb attraction of an isolated pair would be about 0.2 ev.

When an electron trapped in an organic glass is detrapped by light, or tunnels or diffuses and combines with a cation or radical, the energy of combination may appear as luminescence. The spectrum, temperature, and time scale of appearance of the luminescence provide valuable information on the nature of the combination processes involved (73). The migration of trapped charged species as diffusion sets in during warm-up and when electrons are detrapped or detached from anions by light has also been investigated by observing changes in the electrical conductivity of thin samples of organic glasses (74). Measurements of the heats of reaction of electrons, anions, and radicals in organic glasses by differential thermal analysis show promise of yielding information on the energetics of the trapping and combination processes (75).

The theoretical rationalization of the observations that electrons are stabilized in matrices containing cations at concentrations such that each electron experiences a Coulomb attraction greater than its thermal energy, kT, starts with the recognition that there must be potential wells in the matrix where the electron has lower energy than mobile electrons before trapping (76). In nonpolar hydrocarbon glasses there must be volume irregularities propitious for a favorable balance between the repulsive force between electrons and matrix molecules and the attractive force due to electronic polarization [and to the orientation of the weak dipoles (77)]. In more polar matrices the potential wells are deeper as a result of the stronger molecular dipoles. Progress has been made in the theoretical treatment of the observed phenomena, but additional correlation of theory and experiment is needed.

Other Properties of Organic Glasses

In addition to the discovery that organic glasses can provide potential wells for the physical trapping of electrons, trapping studies are producing other new information about matrix properties. This includes the following: (i) mechanisms must exist for the stabilization of positive charge in organic glasses, such stabilization being favored by olefins or other solutes of slightly lower ionization potential than the solute (4–6, 78); (ii) neither electrons nor positively charged species are observed in polycrystalline organic matrices with fewer than ten carbon atoms per molecule (79), indicating that either the electrons or the positive charge or both can migrate readily, with resultant neutralization; (iii) matrices as similar as 3-methylpentane and 3-ethylpentane differ by a factor of 3 in their ability to trap electrons ejected by γ-irradiation (72); and (iv) annealing a 3MP matrix at 77°K for 250 hours after quench cooling before γ-irradiation can change the initial half-life of the decay of trapped electrons by as much as a factor of 5, the initial value and the change depending on the size and shape of the sample (80).

Summary

Free radicals, hydrogen atoms, and electrons produced in rigid organic glasses at sufficiently low temperatures have lifetimes of minutes to years. They can be studied by their electron spin resonance spectra and, in the case of electrons, by their optical spectra, recombination luminescence, and electrical conductivity. The decay kinetics of these reaction intermediates serve to distinguish those trapped as geminate pairs or in spurs of high concentration from those formed with random distributions. Electron spin resonance studies of relaxation times and of the spectra of radical pairs provide further evidence on geometrical distributions. The decay rates of radicals combining with reactive geminate partners are dependent on the size and shape of the radical, the temperature, and the nature of
the matrix. Decay is much slower in deuterated matrices than in protiated matrices. The factors that control the physical trapping of electrons in organic glasses are under intensive investigation. There is evidence that many electrons trapped relatively weakly during irradiations at 4°K deepen their traps by orientation of dipoles when the matrix is warmed; that most electrons are trapped in the field of the geminate positive ion; that in some matrices the traps have a bound excited state to which the electron can be promoted without detrapping; and that trapped electrons can tunnel to solute molecules with a higher electron affinity than the trap depth.

References and Notes

1. For examples and references see: R. G. W. Norrish, in *Nobel Symposium 5, Fast Reactions and Primary Processes in Chemical Kinetics*, S. Claesson, Ed. (Interscience, New York, 1967), pp. 33–70; M. Ebert, J. P. Keene, A. J. Swallow, J. H. Baxendale, *Pulse Radiolysis* (Academic Press, New York, 1965); L. M. Dorfman and M. S. Matheson, in *Progress in Reaction Kinetics*, G. Porter, Ed. (Pergamon, New York, 1965), vol. 3, pp. 237–301; R. K. Wolf, M. J. Bronskill, J. W. Hunt, *J. Chem. Phys.* **53**, 5211 (1970).
2. R. W. Fessenden and R. H. Schuler, *J. Chem. Phys.* **39**, 2147 (1963); E. C. Avery, J. R. Remko, B. Smaller, *ibid.* **49**, 951 (1968).
3. A. M. Bass and H. P. Broida, Eds., *Formation and Trapping of Free Radicals* (Academic Press, New York, 1960).
4. W. H. Hamill, in *Radical Ions*, E. T. Kaiser and L. Kevan, Eds. (Interscience, New York, 1967), pp. 321–416.
5. J. E. Willard, in *Fundamental Processes in Radiation Chemistry*, P. Ausloos, Ed. (Interscience, New York, 1968), pp. 599–649.
6. ———, in *Organic Solid State Chemistry*, G. Adler, Ed. (Gordon & Breach, London, 1969), pp. 135–152; also published in *Mol. Liq. Cryst.* **9**, 135 (1969).
7. L. Kevan, *Actions Chim. Biol. Radiat.* **13**, 57 (1969).
8. ———, *ibid.* **15**, 5 (1971).
9. B. G. Ershov, *ibid.* **14**, 191 (1970).
10. J. Bennett, B. Mile, D. Thomas, B. Ward, *Advan. Phys. Org. Chem.* **8**, 1 (1970).
11. For examples and references see D. E. Milligan and M. E. Jacox, in *Advances in High Temperature Chemistry*, L. Eyring, Ed. (Academic Press, New York, 1971), pp. 1–42.
12. For examples and references see D. A. Ramsay, *Advan. Spectrosc.* **1**, 1 (1959).
13. C. F. Luck and W. Gordy, *J. Amer. Chem. Soc.* **78**, 3240 (1956); W. Gordy and C. G. McCormick, *ibid.*, p. 3243; W. Gordy, *Radiat. Res.* (Suppl. 1) (1959), p. 491. B. Smaller and M. S. Matheson, *J. Chem. Phys.* **28**, 1169 (1958); R. S. Alger, T. H. Anderson, L. A. Webb, *ibid.* **30**, 695 (1959); P. B. Ayscough and C. Thompson, *Trans. Faraday Soc.* **58**, 1477 (1962).
14. W. G. French and J. E. Willard, *J. Phys. Chem.* **72**, 4604 (1968); M. Shirom and J. E. Willard, *ibid.*, p. 1702.
15. R. F. C. Claridge and J. E. Willard, *J. Amer. Chem. Soc.* **87**, 4992 (1965).
16. D. W. Skelly, R. G. Hayes, W. H. Hamill, *J. Chem. Phys.* **43**, 2795 (1965).
17. W. Kam, M. A. Neiss, J. E. Willard, unpublished results.
18. C. R. Roy and J. E. Willard, *J. Phys. Chem.* **76**, 1405 (1972).
19. Throughout this article it has been assumed that the change in height of a line of the first derivative radical spectrum with time is proportional to the change in radical concentration, and that no change in saturation of the ESR signal at 7 mw power occurs during decay. Recent evidence from our laboratory indicates that each of these assumptions may introduce some uncertainty in the quantitative relations between the decays illustrated,

but not in the conclusions as to the major effects of radical and matrix structure.

20. A. C. Ling and J. E. Willard, *J. Phys. Chem.* **72**, 3349 (1968).
21. M. A. Neiss and J. E. Willard, unpublished results.
22. E. D. Sprague and F. Williams, *J. Amer. Chem. Soc.* **93**, 787 (1971); T. Wang and F. Williams, *ibid.* **94**, 2930 (1972); A. Campion and F. Williams, *ibid.*, p. 7633.
23. R. J. LeRoy, E. D. Sprague, F. Williams, *J. Phys. Chem.* **76**, 546 (1972).
24. M. Magat, *Pure Appl. Chem.* **5**, 487 (1962); R. Bensasson, M. Durup, A. Dworkin, M. Magat, R. Marx, H. Szwarc, *Disc. Faraday Soc.* **36**, 177 (1963).
25. H. W. Fenrick, S. V. Filseth, A. L. Hanson, J. E. Willard, *J. Amer. Chem. Soc.* **85**, 3731 (1963); R. J. Egland, P. J. Ogren, J. E. Willard, *J. Phys. Chem.* **75**, 467 (1971).
26. T. Miyazaki, T. Wakayama, K. Fueki, Z. Kuri, *Bull. Chem. Soc. Jap.* **42**, 2086 (1969).
27. D. J. Henderson and J. E. Willard, *J. Amer. Chem. Soc.* **91**, 3014 (1969).
28. Y. Kurita and M. Kashiwagi, *J. Chem. Phys.* **44**, 1727 (1966).
29. R. Arce-Quintero and J. E. Willard, *J. Phys. Chem.* **76**, 1800 (1972).
30. A. Ekstrom, R. D. Suenram, J. E. Willard, *ibid.* **74**, 1888 (1970); D. P. Lin and J. E. Willard, unpublished results.
31. V. K. Ermolaev and V. V. Voevodsky, in *Proceedings of the Second Tihany Symposium on Radiation Chemistry*, J. Dobo and P. Hedvig, Eds. (Hungarian Academy of Sciences, Budapest, 1967), pp. 211–223.
32. H. W. Fenrick, N. B. Nazhat, P. J. Ogren, J. E. Willard, *J. Phys. Chem.* **75**, 472 (1971).
33. K. E. Collins and J. E. Willard, *J. Chem. Phys.* **37**, 1908 (1962).
34. P. J. Ogren, *J. Phys. Chem.* **76**, 1324 (1972).
35. M. Iwasaki, T. Ichikawa, T. Ohmori, *J. Chem. Phys.* **50**, 1984 (1969).
36. ——, *ibid.*, p. 1991.
37. F. Cracco, A. J. Arria, M. Dole, *ibid.* **37**, 2449 (1962).
38. M. Iwasaki and B. Eda, *Chem. Phys. Lett.* **2**, 210 (1968).
39. D. P. Lin, P. Kamlet, L. Kevan, *J. Phys. Chem.* **76**, 1226 (1972); D. P. Lin and L. Kevan, *J. Chem. Phys.* **55**, 2629 (1971).
40. For examples and further references see: M. Iwasaki and K. Toriyama, *J. Chem. Phys.* **47**, 559 (1967); R. H. Johnsen, *J. Phys. Chem.* **65**, 2144 (1961).
41. L. A. Wall, D. W. Brown, R. E. Florin, *J. Phys. Chem.* **63**, 1762 (1959); W. Gordy and R. Morehouse, *Phys. Rev.* **151**, 207 (1966).
42. D. Timm and J. E. Willard, *J. Phys. Chem.* **73**, 2403 (1969).
43. M. A. Long and J. E. Willard, *ibid.* **74**, 1207 (1970).
44. L. Perkey and J. E. Willard, unpublished results.
45. For examples and references see: C. J. Uttee and C. R. Kepford, *J. Chem. Phys.* **52**, 3462 (1970); D. E. Holmes, N. B. Nazhat, J. J. Weiss, *J. Phys. Chem.* **74**, 1622 (1970).
46. For references and correlations of the properties of the stabilized electron in all types of media, see A. Ekstrom, *Radiat. Res. Rev.* **2**, 381 (1970).
47. For references to reviews on the hydrated electron and discussion of its properties, see G. A. Kenney and D. C. Walker, in *Electroanalytical Chemistry*, A. F. Bond, Ed. (Dekker, New York, 1971), vol. 5, pp. 1–66.
48. J. H. Baxendale and P. Wardman, *Nature* **230**, 449 (1971); J. T. Richards and J. K. Thomas, *Chem. Phys. Lett.* **10**, 317 (1971).
49. M. Shirom and J. E. Willard, *J. Amer. Chem. Soc.* **90**, 2184 (1968).
50. S. Fujii and J. E. Willard, *J. Phys. Chem.* **74**, 4313 (1970).
51. J. T. Richards and J. K. Thomas, *J. Chem. Phys.* **53**, 218 (1970).
52. L. Kevan, *ibid.* **56**, 838 (1972).
53. H. Hase, M. Noda, T. Higashimura, *ibid.* **54**, 2975 (1971).
54. D. R. Smith and J. J. Pieroni, *Can. J. Chem.* **45**, 2723 (1967).
55. A. Ekstrom and J. E. Willard, *J. Phys. Chem.* **72**, 4599 (1968).
56. M. J. Blandamer, L. Shields, M. C. R. Symons, *J. Chem. Soc.* (1965), p. 1127.
57. S. Arai and M. C. Sauer, Jr., *J. Chem. Phys.* **44**, 2297 (1966).
58. J. Dyne and O. A. Miller, *Can. J. Chem.* **43**, 2696 (1965).
59. D. W. Skelly and W. H. Hamill, *J. Chem. Phys.* **44**, 2892 (1966).
60. T. Huang, J. Eisele, D. P. Lin, L. Kevan, *ibid.* **56**, 4702 (1972).
61. J. R. Miller and J. E. Willard, *J. Phys. Chem.* **76**, 2341 (1972).
62. D. R. Smith and J. J. Pieroni, *Can. J. Chem.* **43**, 876 (1965).
63. W. M. McClain and A. C. Albrecht, *J. Chem. Phys.* **43**, 465 (1965).
64. K. Tsuji and F. Williams, *J. Phys. Chem.* **72**, 3884 (1968).
65. J. Bullot and A. C. Albrecht, *J. Chem. Phys.* **51**, 2220 (1969).
66. J. R. Miller, *ibid.* **56**, 5173 (1972).
67. J. B. Gallivan and W. H. Hamill, *J. Chem. Phys.* **44**, 1279 (1966); M. Shirom and J. E. Willard, *J. Phys. Chem.* **72**, 1702 (1968).
68. J. R. Miller and J. E. Willard, *J. Phys. Chem.* **76**, 2641 (1972).
69. F. Kieffer, C. Meyer, J. Rigaut, *Chem. Phys. Lett.* **11**, 359 (1971).
70. A. I. Mikhailov, *Dokl. Akad. Nauk SSSR* **197**, 136 (1971); K. I. Zamaraev, R. F. Khairutdinov, A. I. Mikhailov, V. T. Goldanskii, *ibid.* **199**, 640 (1971).
71. H. B. Steen and M. Kongshang, *J. Phys. Chem.* **76**, 2217 (1972).
72. A. Ekstrom, R. Suenram, J. E. Willard, *ibid.* **74**, 1883 (1970).
73. For a critical review of luminescence phenomena in organic glasses, and comprehensive references, see: F. Kieffer and M. Magat, in *Actions Chim. Biol. Radiat.* **14**, 135 (1970); A. Déroulède, F. Kieffer, J. Rigaut, *J. Lumin.* **3**, 325 (1971); B. Brocklehurst, *Radiat. Res. Rev.* **2**, 149 (1970).
74. For reviews and references see: J. E. Willard, *Int. J. Radiat. Phys. Chem.* **4**, 405 (1972); K. F. Bavenstock and P. J. Dyne, *Can. J. Chem.* **48**, 2182 (1970); A. C. Albrecht, *Accounts Chem. Res.* **3**, 238 (1970).
75. M. Nishii, K. Hayashi, S. Okamura, *Nippon Kagaku Zasshi* **82**, 24 (1961); S. Hager and J. E. Willard, unpublished results.
76. For examples and references see: S. A. Rice, *Accounts Chem. Res.* **1**, 81 (1968); D. A. Copeland, N. R. Kestner, J. Jortner, *J. Chem. Phys.* **53**, 1189 (1970); J. Jortner, in *Actions Chim. Biol. Radiat.* **14**, 7 (1970); K. Funabashi and Y. Maruyama, *J. Chem. Phys* **55**, 4494 (1971); A. Albrecht, *Accounts Chem. Res.* **3**, 238 (1970); D. Feng, K. Fueki, L. Kevan, *J. Chem. Phys.* **57**, 1253 (1972); and (46) and (60).
77. D. R. Lide, *J. Chem. Phys.* **46**, 101 (1967).
78. J. P. Guarino and W. H. Hamill, *J. Amer. Chem. Soc.* **86**, 777 (1964); W. F. Louwrier and W. H. Hamill, *J. Phys. Chem.* **74**, 1418 (1970).
79. For examples and references see: A. Ekstrom and J. E. Willard, *J. Phys. Chem.* **74**, 1708 (1970); K. Toriyama and T. Ohmori, *ibid.* **72**, 4347 (1968).
80. D. Shooter and J. E. Willard, *ibid.* **76**, 3167 (1972).
81. R. Fass and J. E. Willard, unpublished results.
82. Work related to the preparation of this article was supported in part by the W. F. Vilas trust of the University of Wisconsin and by USAEC contract AT(11-1)-1715.

Cross-Linking of Collagen

Endogenous aldehydes in collagen react in several ways to form a variety of unique covalent cross-links.

Marvin L. Tanzer

The connective tissue protein, collagen, is the most abundant protein in higher animals where it occurs primarily as extracellular, insoluble fibers. These fibers account for a large part of the organic mass of skin, tendon, blood vessels, bone, teeth, cornea, and vitreous humor. Collagen also provides the framework for most of the parenchymal organs, either in its fibrous form or organized in basement membranes. Because of the ubiquitous distribution and abundance of this structural protein it has been investigated by scientists working in a wide variety of disciplines and specialties ranging from such applied areas as suture production and leather manufacture to the more fundamental aspects of polymer chemistry and the structure-function studies of the protein chemist. In this article I discuss in some detail the structure and function of collagen. In particular I present arguments that (i) the insolubility of collagen fibers is primarily a conseqence of covalent cross-linking; (ii) the covalent cross-links arise from modified amino acids which contain carbonyl groups; and (iii) the molecular packing of collagen monomers into the polymer (fibril) probably specifies which cross-links are formed.

Collagen Behavior

Although all proteins are unique in their structure and action, there are often similarities among proteins which

The author is an associate professor in the Department of Biochemistry, University of Connecticut Health Center, Farmington 06032.